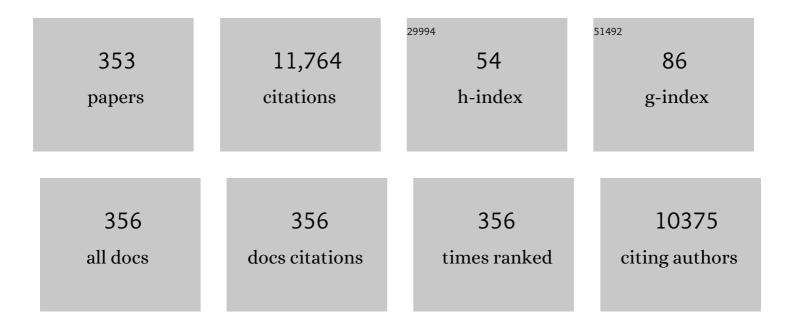
## Xing-Gui Zhou

List of Publications by Year in descending order

Source: https://exaly.com/author-pdf/4663125/publications.pdf Version: 2024-02-01



XINC-CUI ZHOU

#	Article	IF	CITATIONS
1	Probing deactivation by coking in catalyst pellets for dry reforming of methane using a pore network model. Chinese Journal of Chemical Engineering, 2023, 55, 293-303.	1.7	2
2	Mechanistic aspects of facet-dependent CH4/C2+ selectivity over a χ-Fe5C2 Fischer–Tropsch catalyst. Green Energy and Environment, 2022, 7, 449-456.	4.7	8
3	Enhanced recycling performance of bimetallic Ir-Re/SiO2 catalyst by amberlyst-15 for glycerol hydrogenolysis. Chinese Journal of Chemical Engineering, 2022, 45, 171-181.	1.7	1
4	Combining trace Pt with surface silylation to boost Au/uncalcined <scp>TS</scp> â€1 catalyzed propylene epoxidation with <scp>H<sub>2</sub></scp> and <scp>O<sub>2</sub></scp> . AICHE Journal, 2022, 68, e17416.	1.8	4
5	Modeling of propane dehydrogenation combined with chemical looping combustion of hydrogen in a fixed bed reactor. Chinese Journal of Chemical Engineering, 2022, 47, 165-173.	1.7	3
6	Highâ€yield production of <i>p</i> â€diethynylbenzene through consecutive bromination/dehydrobromination in a microreactor system. AICHE Journal, 2022, 68, e17498.	1.8	7
7	On the ensemble requirement of fully selective chemical looping methane partial oxidation over La-Fe-based perovskites. Applied Catalysis B: Environmental, 2022, 301, 120788.	10.8	34
8	Hierarchical pore construction of alumina microrod supports for Pt catalysts toward the enhanced performance of n-heptane reforming. Chemical Engineering Science, 2022, 252, 117286.	1.9	6
9	Novel pharmaceutical cocrystal of lenalidomide with nicotinamide: Structural design, evaluation, and thermal phase transition study. International Journal of Pharmaceutics, 2022, 613, 121394.	2.6	8
10	Mechanistic insights into acid-affected hydrogenolysis of glycerol to 1,3-propanediol over an Ir–Re/SiO2 catalyst. Chemical Communications, 2022, , .	2.2	2
11	Rational design of heterogeneous catalysts by breaking and rebuilding scaling relations. Chinese Journal of Chemical Engineering, 2022, 41, 22-28.	1.7	3
12	Thermodynamics of Carbon Monoxide Adsorption on Cu/SBA-15 Catalysts: Under Vacuum versus under Atmospheric Pressures. Journal of Physical Chemistry C, 2022, 126, 3078-3086.	1.5	5
13	Molecular‣evel Insights into the Notorious CO Poisoning of Platinum Catalyst. Angewandte Chemie - International Edition, 2022, 61, .	7.2	30
14	Pt-O4 moiety induced electron localization toward In2O-Triggered acetylene Semi-Hydrogenation. Journal of Catalysis, 2022, 407, 290-299.	3.1	9
15	Crystalâ€size–dependent external surface diffusion barriers in Pt/ <scp>ZSM</scp> â€5 catalyzed <i>n</i> â€pentane isomerization. AICHE Journal, 2022, 68, .	1.8	3
16	Catalyst particle shapes and pore structure engineering for hydrodesulfurization and hydrodenitrogenation reactions. Frontiers of Chemical Science and Engineering, 2022, 16, 897-908.	2.3	5
17	Computer-aided bimetallic catalyst screening for ester selective hydrogenation. Catalysis Science and Technology, 2022, 12, 2761-2765.	2.1	2
18	Taming Electrons in Pt/C Catalysts to Boost the Mesokinetics of Hydrogen Production. Engineering, 2022, 14, 124-133.	3.2	1

#	Article	IF	CITATIONS
19	Reducing External Surface Diffusion Barriers by Chemical Vapor Deposition for Improved Zeolite Catalysis. Industrial & Engineering Chemistry Research, 2022, 61, 5747-5756.	1.8	1
20	A Mechanistic Study of Oxygen Replenishment of Reduced Perovskites in Chemical Looping Redox Reactions. Journal of Physical Chemistry C, 2022, 126, 7431-7445.	1.5	3
21	Size Dependence of Pd-Catalyzed Hydrogenation of 2,6-Diamino-3,5-dinitropyridine. Industrial & Engineering Chemistry Research, 2022, 61, 6427-6435.	1.8	5
22	Engineering Pore Network Structure of Binders for Improved Catalytic Performance of Zeolite Pellets Using a Multiscale Model. Industrial & Engineering Chemistry Research, 2022, 61, 6354-6366.	1.8	2
23	Enhanced catalytic performance of transition metal-doped Cr2O3 catalysts for propane dehydrogenation: A microkinetic modeling study. Chemical Engineering Journal, 2022, 446, 136913.	6.6	4
24	Enhanced acetylene semi-hydrogenation on a subsurface carbon tailored Ni–Ga intermetallic catalyst. Journal of Materials Chemistry A, 2022, 10, 19722-19731.	5.2	17
25	Probing the structure sensitivity of dimethyl oxalate partial hydrogenation over Ag nanoparticles: A combined experimental and microkinetic study. Chemical Engineering Science, 2022, 259, 117830.	1.9	9
26	Platelet carbon nanofibers as support of Pt-CoO electrocatalyst for superior hydrogen evolution. Journal of Energy Chemistry, 2021, 52, 33-40.	7.1	20
27	Crucial size effects of atomic-layer-deposited Pt catalysts on methanol electrooxidation. Catalysis Today, 2021, 364, 157-163.	2.2	15
28	Support effects of Cs/Al2O3 catalyzed aldol condensation of methyl acetate with formaldehyde. Catalysis Today, 2021, 365, 310-317.	2.2	27
29	Tailoring catalytic properties of V2O3 to propane dehydrogenation through single-atom doping: A DFT study. Catalysis Today, 2021, 368, 46-57.	2.2	29
30	Crucial roles of support modification and promoter introduction in Fe/CNT catalyzed syngas conversion to lower olefins. Catalysis Today, 2021, 368, 126-132.	2.2	5
31	A Supervised Adaptive Resampling Monitoring Method for Quality Indicator in Time-Varying Process. IEEE Transactions on Instrumentation and Measurement, 2021, 70, 1-10.	2.4	9
32	Integrated Reactor ombustor Recycling System for Safe Operation by Catalytic Removal of Excess O 2. Chemical Engineering and Technology, 2021, 44, 670-680.	0.9	1
33	Optimizing catalyst supports at single catalyst pellet and packed bed reactor levels: A comparison study. AICHE Journal, 2021, 67, e17163.	1.8	11
34	Design and tailoring of advanced catalytic process for light alkanes upgrading. EcoMat, 2021, 3, e12095.	6.8	10
35	Rational Design of Single-Atom-Doped Ga <sub>2</sub> O <sub>3</sub> Catalysts for Propane Dehydrogenation: Breaking through Volcano Plot by Lewis Acid–Base Interactions. ACS Catalysis, 2021, 11, 5135-5147.	5.5	41
36	Effect of External Surface Diffusion Barriers on Platinum/Beta atalyzed Isomerization of n â€Pentane. Angewandte Chemie, 2021, 133, 14515-14519.	1.6	8

#	Article	IF	CITATIONS
37	Optimization of catalyst pellet structures and operation conditions for CO methanation. Chinese Journal of Chemical Engineering, 2021, 40, 106-113.	1.7	4
38	Effect of External Surface Diffusion Barriers on Platinum/Betaâ€Catalyzed Isomerization of <i>n</i> â€Pentane. Angewandte Chemie - International Edition, 2021, 60, 14394-14398.	7.2	34
39	Engineering Ru atomic structures toward enhanced kinetics of hydrogen generation. Chemical Engineering Science, 2021, 235, 116507.	1.9	6
40	Kinetics decoupling activity and selectivity of Pt nanocatalyst for enhanced glycerol oxidation performance. AICHE Journal, 2021, 67, e17339.	1.8	5
41	Optimal design of hierarchically structured <scp>ZSM</scp> â€5 zeolites for <scp><i>n</i>â€hexane</scp> isomerization. AICHE Journal, 2021, 67, e17355.	1.8	7
42	Effects of Oxygen Vacancy and Pt Doping on the Catalytic Performance of <scp>CeO<sub>2</sub></scp> in Propane Dehydrogenation: A <scp>Firstâ€Principles</scp> Study. Chinese Journal of Chemistry, 2021, 39, 2391-2402.	2.6	13
43	High-Throughput Screening of Alloy Catalysts for Dry Methane Reforming. ACS Catalysis, 2021, 11, 8881-8894.	5.5	47
44	Liquid Flow and Mass Transfer Behaviors in a Butterfly-Shaped Microreactor. Micromachines, 2021, 12, 883.	1.4	10
45	Mechanism-guided elaboration of ternary Au–Ti–Si sites to boost propylene oxide formation. Chem Catalysis, 2021, 1, 885-895.	2.9	21
46	Understanding size-dependent hydrogenation of dimethyl oxalate to methyl glycolate over Ag catalysts. Journal of Catalysis, 2021, 401, 252-261.	3.1	20
47	Kinetics and mechanistic insights into the hydrothermal synthesis of alumina microrods. Chemical Engineering Science, 2021, 244, 116817.	1.9	7
48	Systematic thermodynamic study of clorsulon dissolved in ten organic solvents: Mechanism evaluation by modeling and molecular dynamic simulation. Journal of Molecular Liquids, 2021, 341, 117217.	2.3	9
49	Rational design of intermetallic compound catalysts for propane dehydrogenation from a descriptor-based microkinetic analysis. Journal of Catalysis, 2021, 404, 32-45.	3.1	15
50	Structural and Kinetics Understanding of Support Effects in Pd-Catalyzed Semi-Hydrogenation of Acetylene. Engineering, 2021, 7, 103-110.	3.2	36
51	Thermodynamics Insights into the Selective Hydrogenation of Alkynes in C <sub>2</sub> and C <sub>3</sub> Streams. Industrial & Engineering Chemistry Research, 2021, 60, 16969-16980.	1.8	3
52	Molecular-level insights into the electronic effects in platinum-catalyzed carbon monoxide oxidation. Nature Communications, 2021, 12, 6888.	5.8	18
53	Tuning partially charged Pt <sup><i>δ</i>+</sup> of atomically dispersed Pt catalysts toward superior propane dehydrogenation performance. Catalysis Science and Technology, 2021, 11, 7840-7843.	2.1	5
54	Polyoxometalates-engineered hydrogen generation rate and durability of Pt/CNT catalysts from ammonia borane. Journal of Energy Chemistry, 2020, 41, 142-148.	7.1	26

#	Article	IF	CITATIONS
55	Synergy of carbocatalytic and heat activation of persulfate for evolution of reactive radicals toward metal-free oxidation. Catalysis Today, 2020, 355, 319-324.	2.2	28
56	Propene epoxidation with H2 and O2 on Au/TS-1 catalyst: Cost-effective synthesis of small-sized mesoporous TS-1 and its unique performance. Catalysis Today, 2020, 347, 102-109.	2.2	29
57	Shape selectivity in acidic zeolite catalyzed 2-pentene skeletal isomerization from first principles. Catalysis Today, 2020, 347, 115-123.	2.2	7
58	Active sites engineering of Pt/CNT oxygen reduction catalysts by atomic layer deposition. Journal of Energy Chemistry, 2020, 45, 59-66.	7.1	54
59	Uncalcined TSâ€2 immobilized Au nanoparticles as a bifunctional catalyst to boost direct propylene epoxidation with H <sub>2</sub> and O <sub>2</sub> . AICHE Journal, 2020, 66, e16815.	1.8	31
60	Deactivation and regeneration of Claus catalyst particles unraveled by pore network model. Chemical Engineering Science, 2020, 211, 115305.	1.9	12
61	Active sites of Pt/CNTs nanocatalysts for aerobic base-free oxidation of glycerol. Green Energy and Environment, 2020, 5, 76-82.	4.7	22
62	Tailoring electronic properties and kinetics behaviors of Pd/N NTs catalysts for selective hydrogenation of acetylene. AICHE Journal, 2020, 66, e16857.	1.8	28
63	In-Situ Catalytic Upgrading of Tar and Coke during Biomass/Coal Co-pyrolysis. Industrial & Engineering Chemistry Research, 2020, 59, 17182-17191.	1.8	10
64	Understanding the Role of Internal Diffusion Barriers in Pt/Beta Zeolite Catalyzed Isomerization of <i>n</i> â€Heptane. Angewandte Chemie, 2020, 132, 1564-1567.	1.6	24
65	Understanding the Role of Internal Diffusion Barriers in Pt/Beta Zeolite Catalyzed Isomerization of <i>n</i> â€Heptane. Angewandte Chemie - International Edition, 2020, 59, 1548-1551.	7.2	37
66	Crystal engineering of hierarchical zeolite in dynamically maintained Pickering emulsion. Chemical Engineering Research and Design, 2020, 153, 49-62.	2.7	8
67	Unprecedented yield of methyl-esterification with in-situ generated diazomethane in a microchannel reactor with methanol as solvent. Chemical Engineering Science, 2020, 213, 115397.	1.9	6
68	Dry reforming of methane on Ni-Fe-MgO catalysts: Influence of Fe on carbon-resistant property and kinetics. Applied Catalysis B: Environmental, 2020, 264, 118497.	10.8	122
69	Solubility and thermodynamics of d-glucosamine 2-sulfate sodium salt in water and binary solvent mixtures with methanol, ethanol and n-propanol. Journal of Molecular Liquids, 2020, 300, 112218.	2.3	10
70	Catalyst consisting of Ag nanoparticles anchored on amine-derivatized mesoporous silica nanospheres for the selective hydrogenation of dimethyl oxalate to methyl glycolate. Journal of Catalysis, 2020, 391, 155-162.	3.1	18
71	Bi-reforming of methane with steam and CO <sub>2</sub> under pressurized conditions on a durable Ir–Ni/MgAl <sub>2</sub> O <sub>4</sub> catalyst. Chemical Communications, 2020, 56, 13536-13539.	2.2	24
72	Size Dependence of Pt Catalysts for Propane Dehydrogenation: from Atomically Dispersed to Nanoparticles. ACS Catalysis, 2020, 10, 12932-12942.	5.5	144

#	Article	IF	CITATIONS
73	Role of Câ€Defective Sites in CO Adsorption over ϵâ€Fe 2 C and ηâ€Fe 2 C Fischerâ€Tropsch Catalysts. Chemistry an Asian Journal, 2020, 15, 4014-4022.	<sup>7</sup> ī.7	9
74	How PM2.5 Affects Pt-Catalyzed Oxygen Reduction Reaction. ACS Sustainable Chemistry and Engineering, 2020, 8, 9385-9392.	3.2	5
75	Beyond the Reverse Horiuti–Polanyi Mechanism in Propane Dehydrogenation over Pt Catalysts. ACS Catalysis, 2020, 10, 14887-14902.	5.5	44
76	Direct and Efficient Synthesis of Clean H <sub>2</sub> O <sub>2</sub> from CO-Assisted Aqueous O <sub>2</sub> Reduction. ACS Catalysis, 2020, 10, 13993-14005.	5.5	9
77	Atomic Insights into Robust Pt–PdO Interfacial Site-Boosted Hydrogen Generation. ACS Catalysis, 2020, 10, 11417-11429.	5.5	19
78	Identification of Synergistic Actions between Cu <sup>0</sup> and Cu <sup>+</sup> Sites in Hydrogenation of Dimethyl Oxalate from Microkinetic Analysis. Industrial & Engineering Chemistry Research, 2020, 59, 22451-22459.	1.8	11
79	A pore network model for calculating pressure drop in packed beds of arbitraryâ€shaped particles. AICHE Journal, 2020, 66, e16258.	1.8	8
80	Rational screening of single-atom-doped ZnO catalysts for propane dehydrogenation from microkinetic analysis. Catalysis Science and Technology, 2020, 10, 4938-4951.	2.1	18
81	Active sites and reaction mechanism for N-doped carbocatalysis of phenol removal. Green Energy and Environment, 2020, 5, 444-452.	4.7	20
82	Elucidating the methanol conversion in H-SAPO-5 from first principles: Nature of hydrocarbon pool and scission style. Molecular Catalysis, 2020, 490, 110948.	1.0	4
83	Synergistic Pt-WO3 Dual Active Sites to Boost Hydrogen Production from Ammonia Borane. IScience, 2020, 23, 100922.	1.9	35
84	Zeolite crystal size effects of Au/uncalcined TS-1 bifunctional catalysts on direct propylene epoxidation with H2 and O2. Chemical Engineering Science, 2020, 227, 115907.	1.9	28
85	On the nature of Pt-carbon interactions for enhanced hydrogen generation. Journal of Catalysis, 2020, 389, 492-501.	3.1	17
86	Kinetic Study of the Hydrogenation of Unsaturated Aldehydes Promoted by CuPt <sub><i>x</i></sub> /SBA-15 Single-Atom Alloy (SAA) Catalysts. ACS Catalysis, 2020, 10, 3431-3443.	5.5	53
87	Heat integrated technology assisted pressure-swing distillation for the mixture of ethylene glycol and 1,2-butanediol. Separation and Purification Technology, 2020, 241, 116740.	3.9	25
88	Coupling non-isothermal trickle-bed reactor with catalyst pellet models to understand the reaction and diffusion in gas oil hydrodesulfurization. Chinese Journal of Chemical Engineering, 2020, 28, 1095-1106.	1.7	9
89	Adsorption Site Regulation to Guide Atomic Design of Ni–Ga Catalysts for Acetylene Semiâ€Hydrogenation. Angewandte Chemie - International Edition, 2020, 59, 11647-11652.	7.2	111
90	Polymer decoration of carbon support to boost Pt-catalyzed hydrogen generation activity and durability. Journal of Catalysis, 2020, 385, 289-299.	3.1	7

#	Article	IF	CITATIONS
91	Dualâ€function catalysis in propane dehydrogenation over <scp>Pt<sub>1</sub>–Ga<sub>2</sub>O<sub>3</sub></scp> catalyst: Insights from a microkinetic analysis. AICHE Journal, 2020, 66, e16232.	1.8	27
92	Adsorption Site Regulation to Guide Atomic Design of Ni–Ga Catalysts for Acetylene Semiâ€Hydrogenation. Angewandte Chemie, 2020, 132, 11744-11749.	1.6	31
93	Aluminous ZSM-48 Zeolite Synthesis Using a Hydroisomerization Intermediate Mimicking Allyltrimethylammonium Chloride as a Structure-Directing Agent. Industrial & Engineering Chemistry Research, 2020, 59, 11139-11148.	1.8	18
94	Methyl Methacrylate Synthesis: Thermodynamic Analysis for Oxidative Esterification of Methacrolein and Aldol Condensation of Methyl Acetate. Industrial & Engineering Chemistry Research, 2020, 59, 17408-17416.	1.8	17
95	Jet Fuel Range Hydrocarbon Production from Propanal: Mechanistic Insights into Active Site Requirement of a Dual-Bed Catalyst. ACS Sustainable Chemistry and Engineering, 2020, 8, 9434-9446.	3.2	5
96	Hierarchical NiCo LDH–rGO/Ni Foam Composite as Electrode Material for High-Performance Supercapacitors. Transactions of Tianjin University, 2019, 25, 266-275.	3.3	17
97	Understanding of two-stage continuous microreaction technology for in-situ generation and consecutive conversion of diazomethane. Journal of the Taiwan Institute of Chemical Engineers, 2019, 98, 94-98.	2.7	4
98	Site-Dependent Activity and Selectivity of H <sub>2</sub> O <sub>2</sub> Formation from H <sub>2</sub> and O <sub>2</sub> over Au-Based Catalysts. Industrial & Engineering Chemistry Research, 2019, 58, 15119-15126.	1.8	15
99	Thermal stability of nanoparticle supported on Al2O3 with different morphologies. Materials Research Express, 2019, 6, 095064.	0.8	1
100	Process simulation and optimization of propane dehydrogenation combined with selective hydrogen combustion. Chemical Engineering and Processing: Process Intensification, 2019, 143, 107608.	1.8	8
101	An analytical method for the optimization of pore network in lithium-ion battery electrodes. Chemical Engineering Research and Design, 2019, 149, 226-234.	2.7	7
102	Size-Dependent Segregation Preference in Single-Atom Alloys of Late Transition Metals: Effects of Magnetism, Electron Correlation, and Geometrical Strain. Journal of Physical Chemistry C, 2019, 123, 18417-18424.	1.5	8
103	Role of electronic properties in partition of radical and nonradical processes of carbocatalysis toward peroxymonosulfate activation. Carbon, 2019, 153, 73-80.	5.4	93
104	CO Adsorption and Activation of Î-Fe <sub>2</sub> C Fischer–Tropsch Catalyst. Industrial & Engineering Chemistry Research, 2019, 58, 21296-21303.	1.8	9
105	Boosting HER Performance of Pt-Based Catalysts Immobilized on Functionalized Vulcan Carbon by Atomic Layer Deposition. Frontiers in Materials, 2019, 6, .	1.2	44
106	Origin of Chemisorption Energy Scaling Relations over Perovskite Surfaces. Journal of Physical Chemistry C, 2019, 123, 28275-28283.	1.5	11
107	Surface Engineering and Kinetics Behaviors of Au/Uncalcined TS-1 Catalysts for Propylene Epoxidation with H <sub>2</sub> and O <sub>2</sub> . Industrial & Engineering Chemistry Research, 2019, 58, 17300-17307.	1.8	29
108	Toward rational catalyst design for partial hydrogenation of dimethyl oxalate to methyl glycolate: a descriptor-based microkinetic analysis. Catalysis Science and Technology, 2019, 9, 5763-5773.	2.1	19

#	Article	IF	CITATIONS
109	Controlling Selectivity in Unsaturated Aldehyde Hydrogenation Using Single-Site Alloy Catalysts. ACS Catalysis, 2019, 9, 9150-9157.	5.5	55
110	The role of H <sub>2</sub> S addition on Pt/Al <sub>2</sub> O <sub>3</sub> catalyzed propane dehydrogenation: a mechanistic study. Catalysis Science and Technology, 2019, 9, 867-876.	2.1	21
111	Kinetics-assisted discrimination of active sites in Ru catalyzed hydrolytic dehydrogenation of ammonia borane. Reaction Chemistry and Engineering, 2019, 4, 316-322.	1.9	24
112	Explosion limits estimation and process optimization of direct propylene epoxidation with H2 and O2. Chinese Journal of Chemical Engineering, 2019, 27, 2968-2978.	1.7	4
113	Hydrogenation of acetylenic contaminants over Ni-Based catalyst: Enhanced performance by addition of silver. Journal of Cleaner Production, 2019, 220, 289-297.	4.6	6
114	A phase-transfer crystallization pathway to synthesize ultrasmall silicoaluminophosphate for enhanced catalytic conversion of dimethylether-to-olefin. CrystEngComm, 2019, 21, 577-582.	1.3	10
115	Optimizing catalyst pore network structure in the presence of deactivation by coking. AICHE Journal, 2019, 65, e16687.	1.8	25
116	Process Monitoring via Key Principal Components and Local Information Based Weights. IEEE Access, 2019, 7, 15357-15366.	2.6	9
117	Insights into Hydrogen Transport Behavior on Perovskite Surfaces: Transition from the Grotthuss Mechanism to the Vehicle Mechanism. Langmuir, 2019, 35, 9962-9969.	1.6	29
118	Tuning Adsorption and Catalytic Properties of α-Cr <sub>2</sub> O <sub>3</sub> and ZnO in Propane Dehydrogenation by Creating Oxygen Vacancy and Doping Single Pt Atom: A Comparative First-Principles Study. Industrial & Engineering Chemistry Research, 2019, 58, 10199-10209.	1.8	38
119	Surface phase diagrams of La-based perovskites towards the O-rich limit from first principles. Physical Chemistry Chemical Physics, 2019, 21, 12859-12871.	1.3	7
120	Pickering emulsion mediated crystallization of hierarchical zeolite SSZ-13 with enhanced NH3 selective catalytic reduction performance. Microporous and Mesoporous Materials, 2019, 285, 202-214.	2.2	14
121	Engineering the Hierarchical Pore Structures and Geometries of Hydrodemetallization Catalyst Pellets. Industrial & Engineering Chemistry Research, 2019, 58, 9829-9837.	1.8	15
122	Enhanced performance of catalyst pellets for methane dry reforming by engineering pore network structure. Chemical Engineering Journal, 2019, 373, 1389-1396.	6.6	22
123	Determination of Ternary Vapor–Liquid Equilibrium of Dimethyl Oxalate–Methanol-1,2-Butanediol under Atmosphere Pressure. Journal of Chemical & Engineering Data, 2019, 64, 1349-1356.	1.0	3
124	BEEF-vdW+ <i>U</i> method applied to perovskites: thermodynamic, structural, electronic, and magnetic properties. Journal of Physics Condensed Matter, 2019, 31, 145901.	0.7	11
125	Mechanistic Understanding of Sizeâ€Dependent Oxygen Reduction Activity and Selectivity over Pt/CNT Nanocatalysts. European Journal of Inorganic Chemistry, 2019, 2019, 3210-3217.	1.0	18
126	Pore engineering of hierarchically structured hydrodemetallization catalyst pellets in a fixed bed reactor. Chemical Engineering Science, 2019, 202, 336-346.	1.9	15

#	Article	IF	CITATIONS
127	Reaction mechanism and kinetics for Pt/CNTs catalyzed base-free oxidation of glycerol. Chemical Engineering Science, 2019, 203, 228-236.	1.9	32
128	Promotional effect of Ce and Fe addition on Cu-based extruded catalyst for catalytic elimination of co-fed acrylonitrile and HCN. Catalysis Communications, 2019, 123, 27-31.	1.6	11
129	Distribution Characteristics of Coking Products and Mechanism of Tar Lightening in Preparation of High-Strength Gasification-Coke with Low-Rank Coal Blending. Energy & Fuels, 2019, 33, 10904-10912.	2.5	1
130	Performance-Indicator-Oriented Concurrent Subspace Process Monitoring Method. IEEE Transactions on Industrial Electronics, 2019, 66, 5535-5545.	5.2	69
131	Cost-efficient core-shell TS-1/silicalite-1 supported Au catalysts: Towards enhanced stability for propene epoxidation with H2 and O2. Chemical Engineering Journal, 2019, 377, 119927.	6.6	35
132	Solvent Screening and Process Optimization for Separating Propylene Oxide from Direct Propylene Epoxidation with H2 and O2. Industrial & amp; Engineering Chemistry Research, 2019, 58, 395-402.	1.8	1
133	Electronic Origin of Oxygen Transport Behavior in La-Based Perovskites: A Density Functional Theory Study. Journal of Physical Chemistry C, 2019, 123, 275-290.	1.5	25
134	Balancing the Microâ€Mesoporosity for Activity Maximization of Nâ€Doped Carbonaceous Electrocatalysts for the Oxygen Reduction Reaction. ChemSusChem, 2019, 12, 1017-1025.	3.6	53
135	Enhanced stability for propene epoxidation with H2 and O2 over wormhole-like hierarchical TS-1 supported Au nanocatalyst. Chemical Engineering Journal, 2019, 377, 119954.	6.6	46
136	Fabricating ZSM-23 with reduced aspect ratio through ball-milling and recrystallization: Synthesis, structure and catalytic performance in N-heptane hydroisomerization. Catalysis Today, 2019, 329, 82-93.	2.2	27
137	Kinetics Insights and Active Sites Discrimination of Pd-Catalyzed Selective Hydrogenation of Acetylene. Industrial & Engineering Chemistry Research, 2019, 58, 1888-1895.	1.8	34
138	A comprehensive kinetics study on non-isothermal pyrolysis of kerogen from Green River oil shale. Chemical Engineering Journal, 2019, 377, 120275.	6.6	46
139	Pore network modeling of catalyst deactivation by coking, from single site to particle, during propane dehydrogenation. AICHE Journal, 2019, 65, 140-150.	1.8	43
140	Improved selectivity and coke resistance of core-shell alloy catalysts for propane dehydrogenation from first principles and microkinetic analysis. Chemical Engineering Journal, 2019, 377, 120049.	6.6	42
141	Charge-Tuned CO Activation over a χ-Fe <sub>5</sub> C <sub>2</sub> Fischer–Tropsch Catalyst. ACS Catalysis, 2018, 8, 2709-2714.	5.5	70
142	Effects of zeolite particle size and internal grain boundaries on Pt/Beta catalyzed isomerization of n-pentane. Journal of Catalysis, 2018, 360, 152-159.	3.1	76
143	Synthesis of Nanosized SAPO-34 via an Azeotrope Evaporation and Dry Gel Conversion Route and Its Catalytic Performance in Chloromethane Conversion. Industrial & Engineering Chemistry Research, 2018, 57, 548-558.	1.8	19
144	Effects of methylating agent and BrÃ,nsted acidity on methylation activity of olefins in CHA-structured zeolites: A periodic DFT study. Molecular Catalysis, 2018, 446, 106-114.	1.0	4

#	Article	IF	CITATIONS
145	A single source method to generate Ru-Ni-MgO catalysts for methane dry reforming and the kinetic effect of Ru on carbon deposition and gasification. Applied Catalysis B: Environmental, 2018, 233, 143-159.	10.8	79
146	Decoding Atomic-Level Structures of the Interface between Pt Sub-nanocrystals and Nanostructured Carbon. Journal of Physical Chemistry C, 2018, 122, 7166-7178.	1.5	4
147	Structural and kinetic insights into Pt/CNT catalysts during hydrogen generation from ammonia borane. Chemical Engineering Science, 2018, 192, 1242-1251.	1.9	31
148	Manipulating Gold Spatial Location on Titanium Silicalite-1 To Enhance the Catalytic Performance for Direct Propene Epoxidation with H <sub>2</sub> and O <sub>2</sub> . ACS Catalysis, 2018, 8, 10649-10657.	5.5	44
149	Influence of tubular reactor structure and operating conditions on dry reforming of methane. Chemical Engineering Research and Design, 2018, 139, 39-51.	2.7	23
150	Manipulating the mesostructure of silicoaluminophosphate SAPO-11 <i>via</i> tumbling-assisted, oriented assembly crystallization: a pathway to enhance selectivity in hydroisomerization. Catalysis Science and Technology, 2018, 8, 5044-5061.	2.1	29
151	SbO <sub>x</sub> â€promoted pt nanoparticles supported on CNTs as catalysts for baseâ€free oxidation of glycerol to dihydroxyacetone. AICHE Journal, 2018, 64, 3979-3987.	1.8	23
152	The urea-barbituric acid polymorphic co-crystal system: Characterization, thermodynamics and crystallization. Journal of Crystal Growth, 2018, 502, 45-53.	0.7	11
153	Design, modeling, and optimization of a lightweight MeOH-to-H2 processor. International Journal of Hydrogen Energy, 2018, 43, 14451-14465.	3.8	10
154	Boosting Sizeâ€ <del>S</del> elective Hydrogen Combustion in the Presence of Propene Using Controllable Metal Clusters Encapsulated in Zeolite. Angewandte Chemie, 2018, 130, 9918-9922.	1.6	4
155	Enhanced Catalytic Performance for Propene Epoxidation with H <sub>2</sub> and O <sub>2</sub> over Bimetallic Au–Ag/Uncalcined Titanium Silicate-1 Catalysts. ACS Catalysis, 2018, 8, 7799-7808.	5.5	94
156	Tailoring of Fe/MnK-CNTs Composite Catalysts for the Fischer–Tropsch Synthesis of Lower Olefins from Syngas. Industrial & Engineering Chemistry Research, 2018, 57, 11554-11560.	1.8	21
157	Boosting Sizeâ€Selective Hydrogen Combustion in the Presence of Propene Using Controllable Metal Clusters Encapsulated in Zeolite. Angewandte Chemie - International Edition, 2018, 57, 9770-9774.	7.2	34
158	Coke Formation on Pt–Sn/Al <sub>2</sub> O <sub>3</sub> Catalyst for Propane Dehydrogenation. Industrial & Engineering Chemistry Research, 2018, 57, 8647-8654.	1.8	106
159	Crystallization of ATO silicoaluminophosphates nanocrystalline spheroids using a phase-transfer synthetic strategy for n-heptane hydroisomerization. Journal of Catalysis, 2018, 364, 308-327.	3.1	42
160	Design and optimization of an ammonia fuel processing unit for a stand-alone PEM fuel cell power generation system. International Journal of Energy Research, 2017, 41, 877-888.	2.2	9
161	Kinetic modeling on batch-cooling crystallization of zinc lactate: The influence of malic acid. Journal of Crystal Growth, 2017, 463, 162-167.	0.7	3
162	Method for generating pore networks in porous particles of arbitrary shape, and its application to catalytic hydrogenation of benzene. Chemical Engineering Journal, 2017, 329, 56-65.	6.6	22

#	Article	IF	CITATIONS
163	Cobalt-based layered metal compound nanoplatelets for lithium-ion batteries. Materials Letters, 2017, 194, 189-192.	1.3	3
164	Simultaneously Enhanced Stability and Selectivity for Propene Epoxidation with H <sub>2</sub> and O <sub>2</sub> on Au Catalysts Supported on Nano-Crystalline Mesoporous TS-1. ACS Catalysis, 2017, 7, 2668-2675.	5.5	120
165	The tailored synthesis of nanosized SAPO-34 via time-controlled silicon release enabled by an organosilane precursor. Chemical Communications, 2017, 53, 6132-6135.	2.2	21
166	Thermodynamic analysis of the solubility of polymorphic cytarabine in a variety of pure solvents. Fluid Phase Equilibria, 2017, 445, 1-6.	1.4	8
167	Morphology and location manipulation of Fe nanoparticles on carbon nanofibers as catalysts for ammonia decomposition to generate hydrogen. International Journal of Hydrogen Energy, 2017, 42, 17466-17475.	3.8	20
168	New class of two-dimensional bimetallic nanoplatelets for high energy density and electrochemically stable hybrid supercapacitors. Nano Research, 2017, 10, 3018-3034.	5.8	19
169	Selective Hydrogenation of Acetylene over Pd-In/Al <sub>2</sub> O <sub>3</sub> Catalyst: Promotional Effect of Indium and Composition-Dependent Performance. ACS Catalysis, 2017, 7, 7835-7846.	5.5	194
170	Decoding structural complexity in conical carbon nanofibers. Physical Chemistry Chemical Physics, 2017, 19, 14555-14565.	1.3	1
171	Hierarchical Silicoaluminophosphate Catalysts with Enhanced Hydroisomerization Selectivity by Directing the Orientated Assembly of Premanufactured Building Blocks. ACS Catalysis, 2017, 7, 5887-5902.	5.5	87
172	Microporous inert membrane packed-bed reactor for propylene epoxidation with hydrogen and oxygen: Modelling and simulation. Chemical Engineering and Processing: Process Intensification, 2017, 122, 425-433.	1.8	7
173	Mechanistic and kinetic insights into the Pt-Ru synergy during hydrogen generation from ammonia borane over PtRu/CNT nanocatalysts. Journal of Catalysis, 2017, 356, 186-196.	3.1	73
174	Influence of catalyst pore network structure on the hysteresis of multiphase reactions. AICHE Journal, 2017, 63, 78-86.	1.8	15
175	Novel Fe/MnKâ€CNTs nanocomposites as catalysts for direct production of lower olefins from syngas. AICHE Journal, 2017, 63, 154-161.	1.8	16
176	Reaction mechanism and kinetics for hydrolytic dehydrogenation of ammonia borane on a Pt/CNT catalyst. AICHE Journal, 2017, 63, 60-65.	1.8	90
177	Probing the Nature of Surface Barriers on ZSMâ€5 by Surface Modification. Chemie-Ingenieur-Technik, 2017, 89, 1333-1342.	0.4	23
178	Water Effect on Secondary Nucleation ofÂtheÂ <i>β</i> â€Form on the Surface of the <i>α</i> â€Form of <i>L</i> â€Glutamic Acid. Chemical Engineering and Technology, 2016, 39, 1295-1300.	0.9	1
179	Composition of the Green Oil in Hydrogenation of Acetylene over a Commercial Pdâ€Ag/Al <sub>2</sub> O <sub>3</sub> Catalyst. Chemical Engineering and Technology, 2016, 39, 865-873.	0.9	39
180	Understanding Coâ€Mo Catalyzed Ammonia Decomposition: Influence of Calcination Atmosphere and Identification of Active Phase. ChemCatChem, 2016, 8, 938-945.	1.8	46

#	Article	IF	CITATIONS
181	Comparative Study of Clogging in Valve andÂCascade Mixers. Chemical Engineering and Technology, 2016, 39, 1451-1456.	0.9	2
182	Probing pore blocking effects on multiphase reactions within porous catalyst particles using a discrete model. AICHE Journal, 2016, 62, 451-460.	1.8	22
183	Nonclassical from-shell-to-core growth of hierarchically organized SAPO-11 with enhanced catalytic performance in hydroisomerization of n-heptane. RSC Advances, 2016, 6, 32523-32533.	1.7	35
184	Thermal stability of TPA template and size-dependent selectivity of uncalcined TS-1 supportedÂAu catalyst for propene epoxidation with H <sub>2</sub> and O <sub>2</sub> . RSC Advances, 2016, 6, 44050-44056.	1.7	29
185	Supersaturation-dependent polymorphic outcome and transformation rate of <scp>l</scp> -glutamic acid. RSC Advances, 2016, 6, 74700-74703.	1.7	11
186	Understanding supersaturationâ€dependent crystal growth of Lâ€alanine in aqueous solution. Crystal Research and Technology, 2016, 51, 23-29.	0.6	16
187	Iron-based Fischer–Tropsch synthesis of lower olefins: The nature of χ-Fe5C2 catalyst and why and how to introduce promoters. Journal of Energy Chemistry, 2016, 25, 911-916.	7.1	57
188	Au/TSâ€l catalyst for propene epoxidation with H <sub>2</sub> /O <sub>2</sub> : A novel strategy to enhance stability by tuning charging sequence. AICHE Journal, 2016, 62, 3963-3972.	1.8	35
189	Hierarchical MgAl2O4 supported Pt-Sn as a highly thermostable catalyst for propane dehydrogenation. Catalysis Communications, 2016, 84, 85-88.	1.6	28
190	Ni(OH)2 nanowires/graphite foam composite as an advanced supercapacitor electrode with improved cycle performance. International Journal of Hydrogen Energy, 2016, 41, 12136-12145.	3.8	21
191	Fabrication of K-promoted iron/carbon nanotubes composite catalysts for the Fischer–Tropsch synthesis of lower olefins. Journal of Energy Chemistry, 2016, 25, 311-317.	7.1	55
192	Insights into Activated Carbon-Supported Platinum Catalysts for Base-Free Oxidation of Glycerol. Industrial & Engineering Chemistry Research, 2016, 55, 420-427.	1.8	26
193	Unraveling the non-classic crystallization of SAPO-34 in a dry gel system towards controlling meso-structure with the assistance of growth inhibitor: Growth mechanism, hierarchical structure control and catalytic properties. Microporous and Mesoporous Materials, 2016, 225, 74-87.	2.2	41
194	Carbon Nanotubes as Support in the Platinum atalyzed Hydrolytic Dehydrogenation of Ammonia Borane. ChemSusChem, 2015, 8, 2927-2931.	3.6	57
195	Insights into the growth of small-sized SAPO-34 crystals synthesized by a vapor-phase transport method. CrystEngComm, 2015, 17, 3214-3218.	1.3	10
196	Density Functional Theory-Assisted Microkinetic Analysis of Methane Dry Reforming on Ni Catalyst. Industrial & Engineering Chemistry Research, 2015, 54, 5901-5913.	1.8	158
197	Insights into the effects of steam on propane dehydrogenation over a Pt/Al <sub>2</sub> O <sub>3</sub> catalyst. Catalysis Science and Technology, 2015, 5, 3991-4000.	2.1	21
198	Modified carbon nanotubes by KMnO <sub>4</sub> supported iron Fischer–Tropsch catalyst for the direct conversion of syngas to lower olefins. Journal of Materials Chemistry A, 2015, 3, 4560-4567.	5.2	57

#	Article	IF	CITATIONS
199	Correlation of solubility and calculation of thermodynamic properties of guanidine nitrate in different solvents. Fluid Phase Equilibria, 2015, 388, 59-65.	1.4	8
200	Nucleation kinetics of lovastatin in different solvents from metastable zone widths. Chemical Engineering Science, 2015, 133, 62-69.	1.9	29
201	<i>In Situ</i> Formation of Cobalt Oxide Nanocubanes as Efficient Oxygen Evolution Catalysts. Journal of the American Chemical Society, 2015, 137, 4223-4229.	6.6	212
202	Dependence of wall stress ratio on wall friction coefficient during the discharging of a 3D rectangular hopper. Powder Technology, 2015, 284, 326-335.	2.1	18
203	Dynamic control of a selective hydrogenation process with undesired MAPD impurities in the C3-cut streams. Journal of the Taiwan Institute of Chemical Engineers, 2015, 54, 28-36.	2.7	4
204	Tuning the composition of metastable Co Ni Mg100â^'â^'(OH)(OCH3) nanoplates for optimizing robust methane dry reforming catalyst. Journal of Catalysis, 2015, 330, 106-119.	3.1	67
205	Carbon nanotubes as transient inhibitors in steam-assisted crystallization of hierarchical ZSM-5 zeolites. Materials Letters, 2015, 159, 466-469.	1.3	17
206	Optimizing spatial pore-size and porosity distributions of adsorbents for enhanced adsorption and desorption performance. Chemical Engineering Science, 2015, 132, 108-117.	1.9	29
207	Recent advances in synthesis of reshaped Fe and Ni particles at the tips of carbon nanofibers and their catalytic applications. Catalysis Today, 2015, 249, 2-11.	2.2	21
208	Au/TS-1 catalyst prepared by deposition–precipitation method for propene epoxidation with H2/O2: Insights into the effects of slurry aging time and Si/Ti molar ratio. Journal of Catalysis, 2015, 325, 128-135.	3.1	51
209	Hierarchical structured α-Al <sub>2</sub> O <sub>3</sub> supported S-promoted Fe catalysts for direct conversion of syngas to lower olefins. Chemical Communications, 2015, 51, 8853-8856.	2.2	69
210	A solvent evaporation route towards fabrication of hierarchically porous ZSM-11 with highly accessible mesopores. RSC Advances, 2015, 5, 31195-31204.	1.7	26
211	Biochemical composite synthesized by stepwise crosslinking: An efficient platform for one-pot biomass conversion. Journal of Catalysis, 2015, 327, 78-85.	3.1	10
212	Insights into HÃ <b>g</b> g Iron-Carbide-Catalyzed Fischer–Tropsch Synthesis: Suppression of CH <sub>4</sub> Formation and Enhancement of C–C Coupling on χ-Fe <sub>5</sub> C <sub>2</sub> (510). ACS Catalysis, 2015, 5, 2203-2208.	5.5	122
213	Synthesis of platinum/graphene composites by a polyol method: The role of graphite oxide precursor surface chemistry. Carbon, 2015, 89, 93-101.	5.4	19
214	Size-Dependent Reaction Mechanism and Kinetics for Propane Dehydrogenation over Pt Catalysts. ACS Catalysis, 2015, 5, 6310-6319.	5.5	189
215	Kinetics study of C 2+ oxygenates synthesis from syngas over Rh–MnO x /SiO 2 catalysts. Chemical Engineering Science, 2015, 135, 312-322.	1.9	28
216	A hierarchical bulky ZSM-5 zeolite synthesized via glycerol-mediated crystallization using a mesoporous steam-treated dry gel as the precursor. New Journal of Chemistry, 2015, 39, 7777-7780.	1.4	7

#	Article	IF	CITATIONS
217	Insights into Polymorphic Transformation of <scp>l</scp> -Glutamic Acid: A Combined Experimental and Simulation Study. Crystal Growth and Design, 2015, 15, 3602-3608.	1.4	13
218	Selective Oxidation of Hydrogen in the Presence of Propylene over Pt-Based Core–Shell Nanocatalysts. Journal of Physical Chemistry C, 2015, 119, 21386-21394.	1.5	15
219	Manipulating the architecture of zeolite catalysts for enhanced mass transfer. Current Opinion in Chemical Engineering, 2015, 9, 42-48.	3.8	7
220	Support effect on the bimetallic structure of Ir–Re catalysts and their performances in glycerol hydrogenolysis. Journal of Molecular Catalysis A, 2015, 410, 81-88.	4.8	28
221	Effects of pretreatment temperature on bimetallic Ir-Re catalysts for glycerol hydrogenolysis. Chinese Journal of Catalysis, 2015, 36, 1750-1758.	6.9	20
222	A mechanistic basis for the effects of Mn loading on C2+ oxygenates synthesis directly from syngas over Rh–MnO /SiO2 catalysts. Chemical Engineering Science, 2015, 135, 301-311.	1.9	19
223	Au/uncalcined TS-1 catalysts for direct propene epoxidation with H2 and O2: Effects of Si/Ti molar ratio and Au loading. Chemical Engineering Journal, 2015, 278, 234-239.	6.6	64
224	Ir–Re alloy as a highly active catalyst for the hydrogenolysis of glycerol to 1,3-propanediol. Catalysis Science and Technology, 2015, 5, 1540-1547.	2.1	71
225	The promoting role of Ag in Ni-CeO2 catalyzed CH4-CO2 dry reforming reaction. Applied Catalysis B: Environmental, 2015, 165, 43-56.	10.8	140
226	Effect of steam addition on the structure and activity of Pt–Sn catalysts in propane dehydrogenation. Chemical Engineering Journal, 2015, 278, 240-248.	6.6	54
227	Tailoring the Structure of Hierarchically Porous Zeolite Beta through Modified Orientated Attachment Growth in a Dry Gel System. Chemistry - A European Journal, 2014, 20, 14744-14755.	1.7	21
228	Evaluation of approximations for concentration-dependent micropore diffusion in sorbent with bidisperse pore structure. Adsorption, 2014, 20, 843-853.	1.4	3
229	Au nanoparticles deposited on the external surfaces of TS-1: Enhanced stability and activity for direct propylene epoxidation with H2 and O2. Applied Catalysis B: Environmental, 2014, 150-151, 396-401.	10.8	91
230	Carbon dioxide reforming of methane over promoted NixMg1â^'xO (111) platelet catalyst derived from solvothermal synthesis. Applied Catalysis B: Environmental, 2014, 148-149, 177-190.	10.8	94
231	Kinetics of Catalytic Dehydrogenation of Propane over Pt-Based Catalysts. Advances in Chemical Engineering, 2014, 44, 61-125.	0.5	17
232	Hydrogenolysis of sorbitol to glycols over carbon nanofibers-supported ruthenium catalyst: The role of base promoter. Chinese Journal of Catalysis, 2014, 35, 692-702.	6.9	21
233	Controlling and Formation Mechanism of Oxygen-Containing Groups on Graphite Oxide. Industrial & Engineering Chemistry Research, 2014, 53, 253-258.	1.8	56
234	Mechanistic Insight into Size-Dependent Activity and Durability in Pt/CNT Catalyzed Hydrolytic Dehydrogenation of Ammonia Borane. Journal of the American Chemical Society, 2014, 136, 16736-16739.	6.6	273

#	Article	IF	CITATIONS
235	Size Effects of Pt Nanoparticles Supported on Carbon Nanotubes for Selective Oxidation of Glycerol in a Base-Free Condition. Industrial & Engineering Chemistry Research, 2014, 53, 16309-16315.	1.8	35
236	Unique reactivity in Pt/CNT catalyzed hydrolytic dehydrogenation of ammonia borane. Chemical Communications, 2014, 50, 2142.	2.2	207
237	Evolution of Carbon Nanofiber-Supported Pt Nanoparticles of Different Particle Sizes: A Molecular Dynamics Study. Journal of Physical Chemistry C, 2014, 118, 23711-23722.	1.5	19
238	Synthesis of hierarchically porous ZSM-5 zeolites by steam-assisted crystallization of dry gels silanized with short-chain organosilanes. New Journal of Chemistry, 2014, 38, 5808-5816.	1.4	36
239	Tuning selectivity and stability in propane dehydrogenation by shaping Pt particles: A combined experimental and DFT study. Journal of Molecular Catalysis A, 2014, 395, 329-336.	4.8	48
240	Towards an efficient CoMo/γ-Al 2 O 3 catalyst using metal amine metallate as an active phase precursor: Enhanced hydrogen production by ammonia decomposition. International Journal of Hydrogen Energy, 2014, 39, 12490-12498.	3.8	69
241	The templating effect of an easily available cationic polymer with widely separated charge centers on the synthesis of a hierarchical ZSM-5 zeolite. Journal of Materials Chemistry A, 2014, 2, 18666-18676.	5.2	16
242	Bis(perfluoro-2-n-propoxyethyl)diacyl peroxide initiated homopolymerization of vinylidene fluoride (VDF) and copolymerization with perfluoro-n-propylvinylether (PPVE). Polymer, 2014, 55, 3557-3563.	1.8	4
243	CO Activation Pathways of Fischer–Tropsch Synthesis on χ-Fe5C2 (510): Direct versus Hydrogen-Assisted CO Dissociation. Journal of Physical Chemistry C, 2014, 118, 10170-10176.	1.5	104
244	Size effects of Pt-Re bimetallic catalysts for glycerol hydrogenolysis. Catalysis Today, 2014, 234, 208-214.	2.2	34
245	Insights into size-dependent activity and active sites of Au nanoparticles supported on TS-1 for propene epoxidation with H2 and O2. Journal of Catalysis, 2014, 317, 99-104.	3.1	85
246	Synthesis of hierarchical ZSM-5 zeolite using CTAB interacting with carboxyl-ended organosilane as a mesotemplate. RSC Advances, 2014, 4, 14471.	1.7	30
247	Morphology dependence of catalytic properties of Ni nanoparticles at the tips of carbon nanofibers for ammonia decomposition to generate hydrogen. International Journal of Hydrogen Energy, 2014, 39, 20722-20730.	3.8	16
248	Effects of carbon support on microwave-assisted catalytic dehydrogenation of decalin. Carbon, 2014, 67, 775-783.	5.4	21
249	Effects of Solvent and Impurities on Crystal Morphology of Zinc Lactate Trihydrate. Chinese Journal of Chemical Engineering, 2014, 22, 221-226.	1.7	10
250	Solid–liquid equilibrium of dicyandiamide in different solvents. Fluid Phase Equilibria, 2014, 363, 228-232.	1.4	15
251	Solubility and polymorphic forms of antibiotic lasalocid sodium in different organic solvents. Fluid Phase Equilibria, 2014, 374, 20-24.	1.4	14
252	Hierarchically porous zeolite beta synthesized via steam-assisted crystallization of silanized dry gel. Materials Letters, 2014, 131, 214-216.	1.3	7

#	Article	IF	CITATIONS
253	Carbon mediated catalysis: A review on oxidative dehydrogenation. Chinese Journal of Catalysis, 2014, 35, 824-841.	6.9	78
254	Fe particles on the tops of carbon nanofibers immobilized on structured carbon microfibers for ammonia decomposition. Catalysis Today, 2013, 216, 254-260.	2.2	23
255	Effect of polymorphism on the purity of l-glutamic acid. Journal of Crystal Growth, 2013, 373, 78-81.	0.7	9
256	A unique method to fabricate NixMg1â^'xO (111) nano-platelet solid solution catalyst for CH4-CO2 dry reforming. Catalysis Communications, 2013, 34, 11-15.	1.6	26
257	Structure sensitivity of ammonia decomposition over Ni catalysts: A computational and experimental study. Fuel Processing Technology, 2013, 108, 112-117.	3.7	56
258	Impurity Effect of <scp>l</scp> -Valine on <scp>l</scp> -Alanine Crystal Growth. Crystal Growth and Design, 2013, 13, 1295-1300.	1.4	36
259	Dimensionality-dependent performance of nanostructured bismuth sulfide in photodegradation of organic dyes. Materials Chemistry and Physics, 2013, 138, 755-761.	2.0	21
260	Support effects on catalytic performance for selective combustion of hydrogen in the presence of propene. Fuel Processing Technology, 2013, 108, 82-88.	3.7	8
261	Promotional Effect of Carbon on Fe Catalysts for Ammonia Decomposition: A Density Functional Theory Study. Industrial & Engineering Chemistry Research, 2013, 52, 17151-17155.	1.8	11
262	Adsorption of a single Pt atom on polyaromatic hydrocarbons from first-principle calculations. Chemical Physics Letters, 2013, 575, 76-80.	1.2	8
263	Eco-friendly one-pot synthesis of highly dispersible functionalized graphene nanosheets with free amino groups. Nanotechnology, 2013, 24, 045609.	1.3	35
264	Evolution of Pt Nanoparticles Supported on Fishbone-Type Carbon Nanofibers with Cone–Helix Structures: A Molecular Dynamics Study. Journal of Physical Chemistry C, 2013, 117, 14261-14271.	1.5	10
265	Numerical Reconstruction of the Catalyst Bed Temperature Distribution in a Multitubular Fixed-Bed Reactor by Karhunen–LoÔve Expansion. Industrial & Engineering Chemistry Research, 2013, 52, 7818-7826.	1.8	5
266	Structural manipulation of the catalysts for ammonia decomposition. Catalysis, 2013, , 118-140.	0.6	17
267	In Situ Production of Ni Catalysts at the Tips of Carbon Nanofibers and Application in Catalytic Ammonia Decomposition. Industrial & Engineering Chemistry Research, 2013, 52, 1854-1858.	1.8	31
268	Effect of Zn on the selectivity of Ru in benzene partial hydrogenation from density functional theory investigations. Journal of Molecular Catalysis A, 2013, 370, 44-49.	4.8	5
269	Mass Transfer Intensification in Micro-Fluidic Devices. , 2013, , 113-139.		0
270	MCM-41 supported Co Mo bimetallic catalysts for enhanced hydrogen production by ammonia decomposition. Chemical Engineering Journal, 2012, 207-208, 103-108.	6.6	81

#	Article	IF	CITATIONS
271	Origin of synergistic effect over Ni-based bimetallic surfaces: A density functional theory study. Journal of Chemical Physics, 2012, 137, 014703.	1.2	64
272	First-principles calculations of ammonia decomposition on Ni(110) surface. Surface Science, 2012, 606, 549-553.	0.8	57
273	First-Principles Calculations of Propane Dehydrogenation over PtSn Catalysts. ACS Catalysis, 2012, 2, 1247-1258.	5.5	235
274	Carbon nanofiber supported bimetallic PdAu nanoparticles for formic acid electrooxidation. Journal of Power Sources, 2012, 215, 130-134.	4.0	43
275	Release of interfacial thermal stress and accompanying improvement of interfacial adhesion in carbon fiber reinforced epoxy resin composites: Induced by diblock copolymers. Composites Part A: Applied Science and Manufacturing, 2012, 43, 990-996.	3.8	35
276	Exploiting polymorphism in the purity enhancement of lincomycin hydrochloride. Chemical Engineering Science, 2012, 77, 42-46.	1.9	2
277	Effect of Impurity on the Lateral Crystal Growth of <scp>l</scp> -Alanine: A Combined Simulation and Experimental Study. Industrial & Engineering Chemistry Research, 2012, 51, 14845-14849.	1.8	22
278	Effects of Different Organic Acids on Solubility and Metastable Zone Width of Zinc Lactate. Journal of Chemical & Engineering Data, 2012, 57, 2963-2970.	1.0	12
279	Nickel nanoparticles embedded in the framework of mesoporous TiO2: Efficient and highly stable catalysts for hydrodechlorination of chlorobenzene. Applied Catalysis A: General, 2012, 413-414, 350-357.	2.2	15
280	One-Pot Noninjection Synthesis of Cu-Doped Zn <sub><i>x</i></sub> Cd <sub>1-<i>x</i></sub> S Nanocrystals with Emission Color Tunable over Entire Visible Spectrum. Inorganic Chemistry, 2012, 51, 3579-3587.	1.9	76
281	Modeling of fishbone-type carbon nanofibers with cone-helix structures. Carbon, 2012, 50, 4359-4372.	5.4	39
282	Flat interface mediated synthesis of platelet carbon nanofibers on Fe nanoparticles. Catalysis Today, 2012, 186, 48-53.	2.2	13
283	Effect of Ag on the control of Ni-catalyzed carbon formation: A density functional theory study. Catalysis Today, 2012, 186, 54-62.	2.2	52
284	Controllable synthesis of carbon nanofiber supported Pd catalyst for formic acid electrooxidation. International Journal of Hydrogen Energy, 2012, 37, 7373-7377.	3.8	42
285	Ammonia decomposition on Fe(1 1 0), Co(1 1 1) and Ni(1 1 1) surfaces: A density functional theory study. Journal of Molecular Catalysis A, 2012, 357, 81-86.	4.8	114
286	Hollow Pt-Ni alloy nanospheres with tunable chamber structure and enhanced activity. Journal of Materials Chemistry, 2011, 21, 18447.	6.7	32
287	DFT study of propane dehydrogenation on Pt catalyst: effects of step sites. Physical Chemistry Chemical Physics, 2011, 13, 3257.	1.3	173
288	Grafting of Poly(n-butylacrylate)-b-poly(2-hydroxyethyl methacrylate) on Carbon Fiber and its Effect on Composite Properties. Polymer-Plastics Technology and Engineering, 2011, 50, 260-265.	1.9	18

#	Article	IF	CITATIONS
289	Pressure Drop and Residence Time Distribution in Carbon-Nanofiber/Graphite-Felt Composite for Single Liquid-Phase Flow. Industrial & Engineering Chemistry Research, 2011, 50, 9431-9436.	1.8	3
290	Palladium Nanoparticles Confined in the Cages of MIL-101: An Efficient Catalyst for the One-Pot Indole Synthesis in Water. ACS Catalysis, 2011, 1, 1604-1612.	5.5	151
291	Single-Crystal Bi <sub>2</sub> S <sub>3</sub> Nanosheets Growing via Attachment–Recrystallization of Nanorods. Inorganic Chemistry, 2011, 50, 7729-7734.	1.9	50
292	Facile Synthesis of Highly Luminescent Mn-Doped ZnS Nanocrystals. Inorganic Chemistry, 2011, 50, 10432-10438.	1.9	89
293	Ultrasonic synthesis of nitrogen-doped carbon nanofibers as platinum catalyst support for oxygen reduction. Journal of Power Sources, 2011, 196, 9356-9360.	4.0	27
294	Preparation of CNF-supported Pt catalysts for hydrogen evolution from decalin. Materials Chemistry and Physics, 2011, 126, 41-45.	2.0	20
295	Hydrodynamics and mass transfer in carbon-nanofiber/graphite-felt composite under two phase flow conditions. Chemical Engineering and Processing: Process Intensification, 2011, 50, 1108-1114.	1.8	2
296	Coke Formation on Pt–Sn/Al2O3 Catalyst in Propane Dehydrogenation: Coke Characterization and Kinetic Study. Topics in Catalysis, 2011, 54, 888-896.	1.3	132
297	A Novel Indiumâ€Boron Amorphous Alloy Mediator for Barbierâ€Type Carbonyl Allylation in Aqueous Medium. Advanced Synthesis and Catalysis, 2011, 353, 2131-2136.	2.1	16
298	Catalytic hydrogenation of benzene to cyclohexene on Ru(0001) from density functional theory investigationsâ~†. Catalysis Today, 2011, 160, 234-241.	2.2	46
299	Gas–liquid mixing in a multi-scale micromixer with arborescence structure. Chemical Engineering Journal, 2011, 167, 475-482.	6.6	20
300	Kinetics of propane dehydrogenation over Pt–Sn/Al2O3 catalyst. Applied Catalysis A: General, 2011, 398, 18-26.	2.2	90
301	Tuning the size and shape of Fe nanoparticles on carbon nanofibers for catalytic ammonia decomposition. Applied Catalysis B: Environmental, 2011, 101, 189-196.	10.8	136
302	Effect of electrode fabrication methods on the electrode performance for ethanol oxidation. Journal of Power Sources, 2011, 196, 159-163.	4.0	15
303	Synthesis of highly dispersed and active palladium/carbon nanofiber catalyst for formic acid electrooxidation. Journal of Power Sources, 2011, 196, 4609-4612.	4.0	33
304	Role of CO2 in ethylbenzene dehydrogenation over Fe2O3(0 0 0 1) from first principles. Journal of Molecular Catalysis A, 2011, 344, 53-61.	4.8	16
305	Toward CH <sub>4</sub> dissociation and C diffusion during Ni/Fe-catalyzed carbon nanofiber growth: A density functional theory study. Journal of Chemical Physics, 2011, 134, 134704.	1.2	30
306	Crystallization of zinc lactate in presence of malic acid. Journal of Crystal Growth, 2010, 312, 2747-2755.	0.7	16

#	Article	IF	CITATIONS
307	First-principles calculations of C diffusion through the surface and subsurface of Ag/Ni(100) and reconstructed Ag/Ni(100). Surface Science, 2010, 604, 186-195.	0.8	8
308	Bi2S3 nanostructures: A new photocatalyst. Nano Research, 2010, 3, 379-386.	5.8	209
309	Carbon nanofibers supported Ru catalyst for sorbitol hydrogenolysis to glycols: Effect of calcination. Korean Journal of Chemical Engineering, 2010, 27, 1412-1418.	1.2	23
310	Facile Synthesis of Monodisperse CdS Nanocrystals via Microreaction. Nanoscale Research Letters, 2010, 5, 130-137.	3.1	45
311	Modeling and Simulation of Coke Combustion Regeneration for Coked Cr2O3/Al2O3 Propane Dehydrogenation Catalyst. Chinese Journal of Chemical Engineering, 2010, 18, 618-625.	1.7	10
312	Synthesis of carbon nanofibers/mica hybrids for antistatic coatings. Materials Letters, 2010, 64, 711-714.	1.3	13
313	Recyclable hollow Pd–Fe nanospheric catalyst for Sonogashira-, Heck-, and Ullmann-type coupling reactions of aryl halide in aqueous media. Journal of Colloid and Interface Science, 2010, 349, 613-619.	5.0	43
314	Continuous synthesis of methyl ethyl ketone peroxide in a microreaction system with concentrated hydrogen peroxide. Journal of Hazardous Materials, 2010, 181, 1024-1030.	6.5	19
315	Density functional study of the chemisorption of C1, C2 and C3 intermediates in propane dissociation on Pt(111). Journal of Molecular Catalysis A, 2010, 321, 42-49.	4.8	77
316	Evaluation of the performance of a constructal mixer with the iodide–iodate reaction system. Chemical Engineering and Processing: Process Intensification, 2010, 49, 628-632.	1.8	14
317	Kinetically controlled synthesis of carbon nanofibers with different morphologies by catalytic CO disproportionation over iron catalyst. Chemical Engineering Science, 2010, 65, 193-200.	1.9	9
318	Electrophoretic deposition of network-like carbon nanofibers as a palladium catalyst support for ethanol oxidation in alkaline media. Carbon, 2010, 48, 3323-3329.	5.4	50
319	Carbon Nanofiber-Supported Ru Catalysts for Hydrogen Evolution by Ammonia Decomposition. Chinese Journal of Catalysis, 2010, 31, 979-986.	6.9	48
320	Pressure Drop of Structured Packing of Carbon Nanofiber Composite. Industrial & Engineering Chemistry Research, 2010, 49, 3944-3951.	1.8	7
321	Numerical Investigation of Constructal Distributors with Different Configurations. Chinese Journal of Chemical Engineering, 2009, 17, 175-178.	1.7	12
322	Structureâ€sensitivity of CH <sub>3</sub> dissociation on Ni(100)from firstâ€principles calculations. Asia-Pacific Journal of Chemical Engineering, 2009, 4, 511-517.	0.8	3
323	Effect of hydrogen on the synthesis of carbon nanofibers by CO disproportionation on ultrafine Fe <sub>3</sub> O <sub>4</sub> . Asia-Pacific Journal of Chemical Engineering, 2009, 4, 590-595.	0.8	0
324	Grafting of polystyrene on carbon nanofibers by introducing a methacrylate unit. Polymer International, 2009, 58, 564-569.	1.6	4

#	Article	IF	CITATIONS
325	DFT studies of dry reforming of methane on Ni catalyst. Catalysis Today, 2009, 148, 260-267.	2.2	320
326	Synthesis and characterization of carbon nanofiber/alumina composite by extrusion casting. Carbon, 2009, 47, 2077-2084.	5.4	6
327	Carbon nanofiber-supported palladium nanoparticles as potential recyclable catalysts for the Heck reaction. Applied Catalysis A: General, 2009, 352, 243-250.	2.2	98
328	Enhanced Distribution and Anchorage of Carbon Nanofibers Grown on Structured Carbon Microfibers. Journal of Physical Chemistry C, 2009, 113, 1301-1307.	1.5	18
329	CNFs-supported Pt catalyst for hydrogen evolution from decalin. Catalysis Communications, 2009, 10, 815-818.	1.6	37
330	Catalytic Vapor Decomposition of Methane over Nickle Catalyst: Growth Rate and the Corresponding Microstructures of Carbon Nanofibers. Journal of Chemical Engineering of Japan, 2009, 42, S204-S211.	0.3	2
331	Oxygen reduction reaction properties of carbon nanofibers: Effect of metal purification. Electrochimica Acta, 2008, 53, 3587-3596.	2.6	19
332	Palladium Catalysts Supported on Fishbone Carbon Nanofibers from Different Carbon Sources. Chinese Journal of Catalysis, 2008, 29, 1107-1112.	6.9	6
333	Carbon Nanofiber-Supported Pd Catalysts for Heck Reaction: Effects of Support Interaction. Chinese Journal of Catalysis, 2008, 29, 1145-1151.	6.9	27
334	Synthesis and characterization of titanium silicate-1 supported on carbon nanofiber. Microporous and Mesoporous Materials, 2008, 108, 311-317.	2.2	24
335	Platinum/carbon nanofiber nanocomposite synthesized by electrophoretic deposition as electrocatalyst for oxygen reduction. Journal of Power Sources, 2008, 175, 211-216.	4.0	35
336	Microstructure effect of carbon nanofiber on electrocatalytic oxygen reduction reaction. Catalysis Today, 2008, 131, 270-277.	2.2	43
337	Experimental study of constructal distributor for flow equidistribution in a mini crossflow heat exchanger (MCHE). Chemical Engineering and Processing: Process Intensification, 2008, 47, 229-236.	1.8	52
338	Experimental investigation of the flow distribution of a 2-dimensional constructal distributor. Experimental Thermal and Fluid Science, 2008, 33, 77-83.	1.5	53
339	First-Principles Study of C Adsorption and Diffusion on the Surfaces and in the Subsurfaces of Nonreconstructed and Reconstructed Ni(100). Journal of Physical Chemistry C, 2007, 111, 3447-3453.	1.5	14
340	Effect of carbon nanofiber microstructure on oxygen reduction activity of supported palladium electrocatalyst. Electrochemistry Communications, 2007, 9, 895-900.	2.3	81
341	Peroxidization of methyl ethyl ketone in a microchannel reactor. Chemical Engineering Science, 2007, 62, 5127-5132.	1.9	26
342	Propylene epoxidation in a microreactor with electric heating. Catalysis Today, 2005, 105, 544-550.	2.2	22

#	Article	IF	CITATIONS
343	Optimization of the fixed-bed reactor for ethylene epoxidation. Chemical Engineering and Processing: Process Intensification, 2005, 44, 1098-1107.	1.8	24
344	Control Vector Parametrization with Karhunenâ^'Loéve Expansion. Industrial & Engineering Chemistry Research, 2004, 43, 127-135.	1.8	2
345	Increasing the Molecular Weight of Poly(L-Lactic Acid) by Solid State Polycondensation in a Closed System. Journal of Polymer Engineering, 2003, 23, .	0.6	10
346	Studies on paired packed-bed electrode reactor: Modeling and experiments. Chemical Engineering Science, 1999, 54, 2969-2977.	1.9	4
347	Simulation and optimization of a coupled reactor/column system for trioxane synthesis. Chemical Engineering Science, 1999, 54, 1353-1358.	1.9	10
348	Optimizing control of a wall-cooled fixed-bed reactor. Chemical Engineering Science, 1999, 54, 2739-2744.	1.9	6
349	A hybrid neural network-first principles model for fixed-bed reactor. Chemical Engineering Science, 1999, 54, 2521-2526.	1.9	36
350	A predictive neural network model based on the karhunenâ€loéave expansion for wallâ€cooled fixedâ€bed reactors. Canadian Journal of Chemical Engineering, 1996, 74, 638-646.	0.9	6
351	Modeling of a fixed-bed reactor using the K-L expansion and neural networks. Chemical Engineering Science, 1996, 51, 2179-2188.	1.9	31
352	Molecular‣evel Insights into the Notorious CO Poisoning of Platinum Catalyst. Angewandte Chemie, 0, , .	1.6	0
353	Effects of SiO2 Deposition on Surface Barriers and Catalytic Activity of Different Zeolites. Catalysis	1.4	0